Optical and Quantum Electronics (2022) 54:792
https://doi.org/10.1007/s11082-022-04216-3

Optical soliton solutions of the Chen–Lee–Liu equation in the presence of perturbation and the effect of the inter-modal dispersion, self-steepening and nonlinear dispersion

Muslum Ozisik[1] · Mustafa Bayram[2] · Aydin Secer[1,2] · Melih Cinar[3]

Received: 18 August 2022 / Accepted: 14 September 2022 / Published online: 30 September 2022

Abstract
In this paper, we have investigated the perturbed Chen–Lee–Liu equation which describes the pulse propagation in the optical fibers, under the impact of the inter-modal dispersion, self-steepening and nonlinear dispersion terms. By using the enhanced modified extended tanh expansion method, bright, singular, periodic singular and periodic bright solitons have been obtained and the effects of the coefficients of the inter-modal dispersion, self-steepening and nonlinear dispersion terms on the soliton's dynamics have been examined in each case. In this respect, the review in the article has not been studied and reported before. The computations throughout this paper have been fulfilled by Maple and also the graphical simulations are demonstrated via Matlab.

Keywords Chen–Lee–Liu model · Modified extended tanh expansion method · DNLSII equation · Optical fiber · Dispersion effect

✉ Mustafa Bayram
mustafabayram@biruni.edu.tr

Muslum Ozisik
ozisik@yildiz.edu.tr

Aydin Secer
asecer@biruni.edu.tr

Melih Cinar
mcinar@yildiz.edu.tr

1 Mathematical Engineering, Yildiz Technical University, Istanbul, Turkey

2 Computer Engineering, Biruni University, Istanbul, Turkey

3 Graduate School of Sciences and Engineering, Yildiz Technical University Esenler, Istanbul, Turkey

1 Introduction

In real life, there are many diverse and complicated physical phenomena that can be best modeled by nonlinear Schrödinger (NLS) equations including higher-order nonlinear and dispersion terms. So, the NLS equations have a widespread application in various branches of natural and engineering sciences. Different forms of the NLS equations have commonly come across in nonlinear optics (Leble and Reichel 2009; Dörfler et al. 2011), quantum mechanics (Ohsumi 2019; Chen et al. 2007), plasma physics (Lee et al. 2007; Do Ó et al. 2009) and telecommunication (Zhou 2014; Yin et al. 2017; Tala-Tebue et al. 2018), etc. So, many researchers focus on solving the equations to interpret the dynamics of the solutions. In the literature, there are many produced methods and their versions called extended, modified, improved and generalized, etc. (Cesar et al. 2022; Hajar et al. 2021, 2022; Tarla et al. 2022; Kalim et al. 2021; Ozdemir et al. 2021; Ali et al. 2022; Cinar et al. 2021, 2022a, b; Mahak and Akram 2019; Liu et al. 2018; Biswas et al. 2016; Biswas and Arshed 2018; Korkmaz et al. 2020; Akbar et al. 2021; Raslan 2017; Tarla et al. 2022; Tariq et al. 2018, 2022a, b; Ozisik et al. 2022a).

One of these equations is the Chen–Lee–Liu (CLL) equation which was introduced in 1979 by Chen et al. (1979, 1987) as follows:

$$i\frac{\partial u}{\partial t}+\alpha_1\frac{\partial^2 u}{\partial x^2}+i\alpha_2|u|^2\frac{\partial u}{\partial x}=0, i=\sqrt{-1}, \tag{1}$$

where $u=u(\mathrm{x},\mathrm{t})$ is a complex-valued function and α_1,α_2 are real values and they come from group velocity dispersion and nonlinear dispersion terms, respectively. Besides t represents the temporal variable and x is the spatial variable which is propagation distance. If it is considered that $\alpha_1=\alpha_2=1$, then Eq. (1) converts into the well-known regular Chen–Lee–Liu form. As it is known that Eq. (1) is also called the second derivative nonlinear Schrödinger equation (DNLSII) (Shuwei et al. 2011; Zhang et al. 2015; Gadzhiev et al. 1986). The CLL equation is important in that it represents a model controlling the propagation of the optical pulse with only a self-steepening effect (SSE) but no self-phase modulation (SPM). Especially in 2007, experimentally revealing the physical interpretation of the optical expression, which the DNLSII equation represents rather than being an equation only theoretically or mathematically, has increased the importance of the CLL equation and pioneered the formation of many forms of the CLL equation. Such as, an integrable coupled derivative NLS equation (Sakovich and Sakovich 2005; Feng 2012), DNLSII equation (Liu et al. 2019; Zhou et al. 2022), an integrable coupled CLL model (Tsuchida and Wadati 1999; Alrashed et al. 2022), perturbed CLL (Esen et al. 2021; Yépez-Martínez 2021), CLL in birefringent fiber (Yildirim 2019), higher-order CLL equation (Zhang et al. 2022), conservation laws of CLL equation Arnous et al. 2022), fractional CLL equation (Hussain et al. 2020; Yusuf et al. 2019). It should also be noted here that DNLSII has a wide range of applications, not only in optics but also in the modeling of weak nonlinear propagating water waves (Guo et al. 2014; Xia et al. 2021; Trulsen et al. 2000).

The Chen–Lee–Liu equation describes the propagation in nonlinear optical fibers (Mohamed et al. 2022; Akinyemi et al. 2021), besides it may appears in meta-materials, optical couplers and optoelectronic devices (Baskonus et al. 2021). In this study, we deal with the dimensionless perturbed Chen–Lee–Liu equation defined as Chen et al. (1979), Biswas (2018):

$$i\frac{\partial u}{\partial t}+\alpha_1\frac{\partial^2 u}{\partial x^2}+i\alpha_2|u|^2\frac{\partial u}{\partial x}=i\left(\gamma_1\frac{\partial u}{\partial x}+\gamma_2\frac{\partial\left(|u|^{2n}u\right)}{\partial x}+\gamma_3\frac{\partial|u|^{2n}}{\partial x}u\right),\ i=\sqrt{-1}, \quad (2)$$

where $u=u(x,t)$ is a complex function and the parameters α_1,α_2 are the coefficient of the group velocity dispersion and nonlinear dispersion term, respectively. The coefficients $\gamma_1,\gamma_2,$ and γ_3 are the inter-modal dispersion (IMD), the self-steepening and nonlinear dispersion terms, respectively. In addition, the all parameters are real values and n, the parameter of full nonlinearity, refers the density of complex function.

In the literature, the considered perturbed CLL equation has been solved via some other methods such as the first integral (Kudryashov 2019), Jacobi and the Weierstrass elliptic functions (Kudryashov 2021), Jacobi elliptic function method Tarla et al. (2022), generalized exponential rational function method (Tarla et al. 2022), both modified G/G'-expansion and modified Kudryashov methods (Yokus et al. 2021), the generalized Kudryashov and $\exp(-\varphi(\eta))$-expansion methods (Baskonus et al. 2021). Besides, Yildirim et al. (2020) studied the considered equation by using different techniques that are Riccati, Sine-Gordon, F-Expansion, functional variable, Exp- expansion, trial equation and modified simple equation technique. As can be seen from the references in Yildirim et al. (2020), Kudryashov (2019), Biswas (2018), Kudryashov (2021), Tarla et al. (2022), Tarla et al. (2022), Yokus et al. (2021), Baskonus et al. (2021), the existing studies in the literature generally focus on the existence of some soliton solutions of the perturbed CLL equation with different refractive indexes or obtaining soliton solutions by applying different methods.

The aim of this study is not only focused on the soliton solution of the perturbed CLL equation, but also to examine the effects of terms of the inter-modal, self-steepening and nonlinear dispersion on the soliton behavior represented by the perturbed CLL equation. In this respect, no such review and results presented in this article have been reported for the perturbed CLL equation before.

In this study, the enhanced modified extended tanh expansion method (eMETEM) (Ozisik et al. 2022b) has been applied to construct some soliton solutions of the perturbed CLL equation. Extracting the effects of the coefficients of the inter-modal, self-steepening and nonlinear dispersion terms on soliton dynamics will encourage further studies.

The remaining part is arranged as follows: The algorithm of the method is described in Sect. 2. We apply the proposed method to perturbed CLL equation in Sect. 3. The results of the paper and the plots of the obtained solutions are explained in Sect. 4. We give a conclusion in the final section.

2 Review of the enhanced modified extended tanh expansion method

Step 1: Let us deal with the general form of a NLPDE and the wave transformations, respectively:

$$H\left(U,\frac{\partial U}{\partial t},\frac{\partial U}{\partial x},\frac{\partial^2 U}{\partial t^2},\frac{\partial^2 U}{\partial x^2},\frac{\partial^2 U}{\partial x\partial t},\dots\right)=0, \quad (3)$$

$$U=U(x,t)=Y(\varepsilon),\quad \varepsilon=p_1x+p_2t, \quad (4)$$

Table 1 The solutions of Eq. (7)

$\Psi_1(\varepsilon)=-\sqrt{-\gamma}\tanh\left(\sqrt{-\gamma}(\varepsilon+\varepsilon_0)\right)$,	$\Psi_8(\varepsilon)=\sqrt{\gamma}\tan\left(\sqrt{\gamma}(\varepsilon+\varepsilon_0)\right)$,
$\Psi_2(\varepsilon)=-\sqrt{-\gamma}\coth\left(\sqrt{-\gamma}(\varepsilon+\varepsilon_0)\right)$,	$\Psi_9(\varepsilon)=-\sqrt{\gamma}\cot\left(\sqrt{\gamma}(\varepsilon+\varepsilon_0)\right)$,
$\Psi_3(\varepsilon)=-\sqrt{-\gamma}(\tanh\left(2\sqrt{-\gamma}(\varepsilon+\varepsilon_0)\right)$ $+i\lambda\,\mathrm{sech}\left(2\sqrt{-\gamma}(\varepsilon+\varepsilon_0)\right))$,	$\Psi_{10}(\varepsilon)=\sqrt{\gamma}(\tan\left(2\sqrt{\gamma}(\varepsilon+\varepsilon_0)\right)$ $+\sec\left(2\sqrt{\gamma}(\varepsilon+\varepsilon_0)\right))$,
$\Psi_4(\varepsilon)=\frac{(\gamma-\sqrt{-\gamma}\tanh(\sqrt{-\gamma}(\varepsilon+\varepsilon_0)))}{(1+\sqrt{-\gamma}\tanh(\sqrt{-\gamma}(\varepsilon+\varepsilon_0)))}$,	$\Psi_{11}(\varepsilon)=-\frac{\sqrt{\gamma}(1-\tan(\sqrt{\gamma}(\varepsilon+\varepsilon_0)))}{(1+\tan(\sqrt{\gamma}(\varepsilon+\varepsilon_0)))}$,
$\Psi_5(\varepsilon)=\frac{\sqrt{-\gamma}(5-4\cosh(2\sqrt{-\gamma}(\varepsilon+\varepsilon_0)))}{(3+4\sinh(2\sqrt{-\gamma}(\varepsilon+\varepsilon_0)))}$,	$\Psi_{12}(\varepsilon)=\frac{\sqrt{\gamma}(4-5\cos(2\sqrt{\gamma}(\varepsilon+\varepsilon_0)))}{(3+5\sin(2\sqrt{\gamma}(\varepsilon+\varepsilon_0)))}$,
$\Psi_6(\varepsilon)=\frac{\lambda\sqrt{-\gamma(\alpha^2+\beta^2)}-\alpha\sqrt{-\gamma}\cosh(2\sqrt{-\gamma}(\varepsilon+\varepsilon_0))}{\alpha\sinh(2\sqrt{-\gamma}(\varepsilon+\varepsilon_0))+\beta}$,	$\Psi_{13}(\varepsilon)=\frac{\lambda\sqrt{\gamma(\alpha^2-\beta^2)}-\alpha\sqrt{\gamma}\cos(2\sqrt{\gamma}(\varepsilon+\varepsilon_0))}{\alpha\sin(2\sqrt{\gamma}(\varepsilon+\varepsilon_0))+\beta}$,
$\Psi_7(\varepsilon)=\lambda\sqrt{-\gamma}\left[1-\frac{2\alpha}{\alpha+\cosh(2\sqrt{-\gamma}(\varepsilon+\varepsilon_0))-\lambda\sinh(2\sqrt{-\gamma}(\varepsilon+\varepsilon_0))}\right]$,	$\Psi_{14}(\varepsilon)=i\lambda\sqrt{\gamma}\left[1-\frac{2\alpha}{\alpha+\cos(2\sqrt{\gamma}(\varepsilon+\varepsilon_0))-i\lambda\sin(2\sqrt{\gamma}(\varepsilon+\varepsilon_0))}\right]$,
$\Psi_{15}(\varepsilon)=-\frac{1}{\varepsilon+\varepsilon_0}$ where $\gamma=0$,	

where p_1, p_2 are the wave number and the velocity of the wave, respectively. Substituting the wave transformations in Eq. (4) into Eq. (3), we acquire a nonlinear ordinary differential (ODE) as follows:

$$J\left(Y(\varepsilon), Y'(\varepsilon), Y''(\varepsilon), \dots\right)=0, \tag{5}$$

where the sign $'$ represents the derivatives of $Y(\varepsilon)$ w.r.t. ε.

Step 2: The solutions of the ODE in Eq. (5) can be supposed by the following form:

$$Y(\varepsilon)=A_0+\sum_{i=1}^{m} A_i\Psi^i(\varepsilon)+\sum_{i=1}^{m} B_i\Psi^{-i}(\varepsilon). \tag{6}$$

Here, $A_0, A_1, \dots, A_m, B_1, \dots, B_m$ are real parameters to be determined (A_m and B_m should not be zero, simultaneously) and m is a positive integer to be found by balancing the highest derivative term and the highest power nonlinear term in Eq. (5). Besides, $\Psi(\varepsilon)$ is a function that satisfies the following Riccati differential equation:

$$\frac{d\Psi(\varepsilon)}{d\varepsilon}=\gamma+[\Psi(\varepsilon)]^2, \tag{7}$$

where γ is a nonzero real value.

Step 3: Equation (7) admits the solutions which are given in Table 1.

where γ, α, β and ε_0 are real values and $\lambda=\mp1$.

Step 4: Substituting Eq. (6) and its related derivatives into Eq. 5 and considering Eq. (7), a polynomial in $\Psi(\varepsilon)$ are acquired. Collecting the coefficients of $\Psi(\varepsilon)$ with the same power and equating each coefficient to zero, an algebraic equations system are derived.

Step 5: When the set of algebraic equations in Step 4 is solved, the unknowns $A_0, A_1, \dots, A_m$, $B_1, B_2, \dots, B_m, p_1, p_2, \gamma, \alpha, \beta$ and ε_0 are determined. Substituting the values of the unknowns into Eq. (6) and considering Eq. (4), the solutions of the NLPDE in Eq. (3) are found.

3 Application of the method

Let us take $n = 1$ in the perturbed CLL equation that is given in Eq. (2) and consider the following wave transformation:

$$u(x,t) = e^{i\theta}U(\varepsilon),\ \varepsilon = \eta(x - vt),\ \theta = -kx + \beta t + \varphi, \tag{8}$$

where $U(\varepsilon), \eta, v, \theta, k, \beta$ and φ are the amplitude of the wave, the wave number, velocity, phase component, the frequency, the wave number and phase constant. Substituting the travelling wave transformation in Eq. (8) into Eq. (2), one can obtain real and imaginary parts as follows:

$$\eta^2\alpha_1 U''(\varepsilon) - U(\varepsilon)\big(k\big(\gamma_2 - \alpha_2\big)(U(\varepsilon))^2 + k^2\alpha_1 + k\gamma_1 + \beta\big) = 0, \tag{9}$$

$$-2\eta\big(\big((3/2)\gamma_2 + \gamma_3 - (1/2)\alpha_2\big)(U(\varepsilon))^2 + k\alpha_1 + v/2 + (1/2)\gamma_1\big)U'(\varepsilon) = 0. \tag{10}$$

Integrating the Eq. 10 once and taking the integration constant as zero, we have:

$$-\eta\big(3\gamma_2 + 2\gamma_3\alpha_2\big)(U(\varepsilon))^3 - 3\eta\big(2k\alpha_1 + v + \gamma_1\big)U(\varepsilon) = 0. \tag{11}$$

From Eq. 11, one can get:

$$v = -2k\alpha_1 - \gamma_1, \tag{12}$$

$$\alpha_2 = 3\gamma_2 + 2\gamma_3. \tag{13}$$

Under the constraints in Eqs. (12), (13), we take in to account the Eq. (9) as the ODE representation of Eq. (2):

$$\eta^2\alpha_1 U'' - k\big(\gamma_2 - \alpha_2\big)U^3 - \big(k^2\alpha_1 + k\gamma_1 + \beta\big)U = 0, \tag{14}$$

where $U = U(\varepsilon)$. When we balance the terms U'' and U^3 in Eq. (14) by considering Eq. (6), (7), we attain $m = 1$.

So, the solutions of Eq. (14) are supposed to be a form as follows:

$$U(\varepsilon) = A_0 + A_1\Psi(\varepsilon) + B_1\frac{1}{\Psi(\varepsilon)}. \tag{15}$$

Substituting the Eq. (15) and its derivatives into Eq. (14), we attain the polynomial in $\Psi(\varepsilon)$ by taking Eq. (7) a consideration. Gathering each term with the same power of $\Psi^i(\varepsilon)$ and equating each coefficient to zero, one can get a system of algebraic equation system as:

$$\begin{array}{ll}
\Psi^{-3}(\varepsilon): & B_1\big(k\delta {B_1}^2 + \gamma^2\eta^2\alpha_1\big) = 0,\\
\Psi^{-2}(\varepsilon): & kA_0{B_1}^2\delta = 0,\\
\Psi^{-1}(\varepsilon): & -B_1\big(k^2\alpha_1 + \big(-6A_1\delta B_1 - 6A_0^2\delta + \gamma_1\big)k - 2\gamma\eta^2\alpha_1 + \beta\big) = 0,\\
\Psi^{0}(\varepsilon): & -A_0\big(k^2\alpha_1 + \big(-2\delta A_0^2 - 12A_1B_1(\gamma_2 + \gamma_3) + \gamma_1\big)k + \beta\big) = 0,\\
\Psi^{1}(\varepsilon): & -\big(k^2\alpha_1 + \big(-6A_1\delta B_1 - 6A_0^2\delta) + \gamma_1\big)k - 2\gamma\eta^2\alpha_1 + \beta\big)A_1 = 0,\\
\Psi^{2}(\varepsilon): & kA_0{A_1}^2\delta = 0,\\
\Psi^{3}(\varepsilon): & A_1\big(k\delta {A_1}^2 + \eta^2\alpha_1\big) = 0,
\end{array} \tag{16}$$

where $\delta = \gamma_2 + \gamma_3$.

When we solve the system above by Maple, the unknowns $A_0, A_1, B_1, \alpha_1, \gamma, \gamma_1, \gamma_2, \gamma_3, k$ and β are determined. The some of solution sets are given below:

$$
\begin{aligned}
Cset^1 &= \left\{ \beta = -4\eta^2\gamma\alpha_1 - k^2\alpha_1 - k\gamma_1, A_0 = 0, A_1 = \frac{\eta}{k\delta}\sqrt{-k\delta\alpha_1}, B_1 = \gamma A_1 \right\}, \\
Cset^2 &= \left\{ \beta = \frac{-\eta^2\left(4\gamma\delta^2{A_1}^4 - \gamma_1\delta{A_1}^2 + \eta^2{\alpha_1}^2\right)\alpha_1}{{A_1}^4\delta^2}, k = -\frac{\eta^2\alpha_1}{{A_1}^2\delta}, A_0 = 0, B_1 = \gamma A_1 \right\}, \\
Cset^3 &= \left\{ \beta = \frac{\left(8\gamma\delta^2{A_1}^4 + \gamma_1\delta{A_1}^2 - \eta^2{\alpha_1}^2\right)\eta^2\alpha_1}{{A_1}^4\delta^2}, k = -\frac{\eta^2\alpha_1}{{A_1}^2\delta}, A_0 = 0, B_1 = -\gamma A_1 \right\}.
\end{aligned} \tag{17}
$$

For $j = 1, 2, \dots, 15$, substituting the $\Psi_j(\varepsilon)$ in Table 1 into Eq. (15) and using the sets above, we get the solutions $\Psi_j(\varepsilon)$ of the ODE in Eq. (14). Then, using wave transformations in Eq. (8), we acquire the following solutions $u_j(x,t)$ of the perturbed CLL equation in Eq. (2):

$$u_1(x,t) = \chi\left(A_0 - A_1\sqrt{-\gamma}\tanh\left(\Psi_\tau\right) - \frac{B_1}{\sqrt{-\gamma}\tanh\left(\Psi_\tau\right)} \right), \tag{18}$$

$$u_2(x,t) = \chi\left(A_0 - A_1\sqrt{-\gamma}\coth\left(\Psi_\tau\right) - \frac{B_1}{\sqrt{-\gamma}\coth\left(\Psi_\tau\right)} \right), \tag{19}$$

$$u_3(x,t) = \chi\left(A_0 - A_1\sqrt{-\gamma}\left(\tanh\left(2\Psi_\tau\right) + i\mu\,\mathrm{sech}\left(2\Psi_\tau\right)\right) - \frac{B_1}{\sqrt{-\gamma}\left(\tanh\left(2\Psi_\tau\right) + i\mu\,\mathrm{sech}\left(2\Psi_\tau\right)\right)} \right), \tag{20}$$

$$u_4(x,t) = \chi\left(A_0 + A_1\frac{\gamma - \sqrt{-\gamma}\tanh\left(\Psi_\tau\right)}{1 + \sqrt{-\gamma}\tanh\left(\Psi_\tau\right)} + B_1\frac{1 + \sqrt{-\gamma}\tanh\left(\Psi_\tau\right)}{\gamma - \sqrt{-\gamma}\tanh\left(\Psi_\tau\right)} \right), \tag{21}$$

$$u_5(x,t) = \chi\left(A_0 + A_1\frac{\sqrt{-\gamma}\left(5 - 4\cosh\left(2\Psi_\tau\right)\right)}{3 + 4\sinh\left(2\Psi_\tau\right)} + B_1\frac{3 + 4\sinh\left(2\Psi_\tau\right)}{\sqrt{-w}\left(5 - 4\cosh\left(2\Psi_\tau\right)\right)} \right), \tag{22}$$

$$u_6(x,t) = \chi\left(A_0 + A_1\frac{\mu\sqrt{C_1} - a\sqrt{-\gamma}\cosh\left(2\Psi_\tau\right)}{a\sinh\left(2\Psi_\tau\right) + b} + B_1\frac{a\sinh\left(2\Psi_\tau\right) + b}{\mu\sqrt{C_1} - a\sqrt{-\gamma}\cosh\left(2\Psi_\tau\right)} \right), \tag{23}$$

$$u_7(x,t) = \chi\left[A_0 + A_1\left(\frac{C_2}{a} - \frac{2C_2}{a + \cosh\left(2\Psi_\tau\right) - \mu\sinh\left(2\Psi_\tau\right)} \right) + \frac{B_1}{\frac{C_2}{a} - 2\frac{C_2}{a + \cosh\left(2\Psi_\tau\right) - \mu\sinh\left(2\Psi_\tau\right)}} \right], \tag{24}$$

$$u_8(x,t) = \chi\left(A_0 + A_1\sqrt{\gamma}\tan\left(\Omega_\tau\right) + \frac{B_1}{\sqrt{\gamma}\tan\left(\Omega_\tau\right)} \right), \tag{25}$$

$$u_9(x,t)=\chi\left(A_0-A_1\sqrt{\gamma}\cot\left(\Omega_\tau\right)-\frac{B_1}{\sqrt{\gamma}\cot\left(\Omega_\tau\right)}\right), \tag{26}$$

$$u_{10}(x,t)=\chi\left(A_0+A_1\sqrt{\gamma}\left(\tan\left(2\Omega_\tau\right)+\mu\sec\left(2\Omega_\tau\right)\right)+\frac{B_1}{\sqrt{\gamma}\tan\left(2\Omega_\tau\right)+\mu\sec\left(2\Omega_\tau\right)}\right), \tag{27}$$

$$u_{11}(x,t)=\chi\left(A_0-A_1\frac{\sqrt{\gamma}\left(1-\tan\left(\Omega_\tau\right)\right)}{1+\tan\left(\Omega_\tau\right)}-B_1\frac{1+\tan\left(\Omega_\tau\right)}{\sqrt{\gamma}\left(1-\tan\left(\Omega_\tau\right)\right)}\right), \tag{28}$$

$$u_{12}(x,t)=\chi\left(A_0+A_1\frac{\sqrt{\gamma}\left(4-5\cos\left(2\Omega_\tau\right)\right)}{3+5\sin\left(2\Omega_\tau\right)}+B_1\frac{3+5\sin\left(2\Omega_\tau\right)}{\sqrt{\gamma}\left(4-5\cos\left(2\Omega_\tau\right)\right)}\right), \tag{29}$$

$$u_{13}(x,t)=\chi\left(A_0+A_1\frac{\mu\sqrt{\left(a^2-b^2\right)w}-a\sqrt{w}\cos\left(2\Omega_\tau\right)}{a\sin\left(2\Omega_\tau\right)+b}+B_1\frac{a\sin\left(2\Omega_\tau\right)+b}{\mu\sqrt{\left(a^2-b^2\right)w}-a\sqrt{w}\cos\left(2\Omega_\tau\right)}\right), \tag{30}$$

$$u_{14}(x,t)=\chi\left(A_0+A_1\left(i\mu\sqrt{\gamma}-\frac{2i\mu a\sqrt{\gamma}}{a+\cos\left(2\Omega_\tau\right)-i\mu\sin\left(2\Omega_\tau\right)}\right)+\frac{B_1}{\left(i\mu\sqrt{\gamma}-\frac{2i\mu a\sqrt{\gamma}}{a+\cos\left(2\Omega_\tau\right)-i\mu\sin\left(2\Omega_\tau\right)}\right)}\right), \tag{31}$$

$$u_{15}(x,t)=-\frac{1}{x-vt}, \tag{32}$$

where $\chi=e^{i(\beta t-kx+\phi)}$, $v=-2k\alpha_1-\gamma_1$, $C_1=-\left(a^2+b^2\right)\gamma$, $C_2=\mu a\sqrt{-\gamma}$, $\Omega_\tau=\sqrt{\gamma}\eta(x-vt)$ and $\Psi_\tau=\sqrt{-\gamma}\eta(x-vt)$.

4 Results and discussion

In this paper, we have successfully produced some solutions of the considered equation via the enhanced modified extended tanh expansion method. Besides, the effects of the coefficients of inter-modal dispersion, self-steepening and the nonlinear dispersion terms have been investigated. The codes of the method's algorithm have been written by Maple. Selecting appropriate parameters and using Matlab, we have plotted many graphs of the obtained solutions. To explain the behavior of the obtained solutions, we have created various figures and have made detail interpretations. Each of the given graphics in Figs. 1, 2, 3 and 4 contains 6 sub-figures. These are modulus part in 3D (sub-figure (a)), contour of modulus part in 3D (sub-figure (b)), 2D of modulus part for $t_f=1,2,3$ (solid black to dotted lines), 2D of imaginary part for $t=1$ (blue line) and 2D of the real part for $t=1$ (green line), together in (sub-figure (c)), respectively. The sub-figures (d)–(e)–(f) are the graphs showing the effect of the γ_1,γ_2 and γ_3 on the obtained soliton in sub-figure (a).

Figure 1 is the graph of the combination of $u_3(x,t)$ in Eq. (20) and $Cset^1$ in Eq. (17) for the parameter values $\gamma=-0.1,\gamma_1=\gamma_2=\gamma_3=\varphi=\eta=1,\alpha_1=2,k=-1$. Fig. 1a–c (black

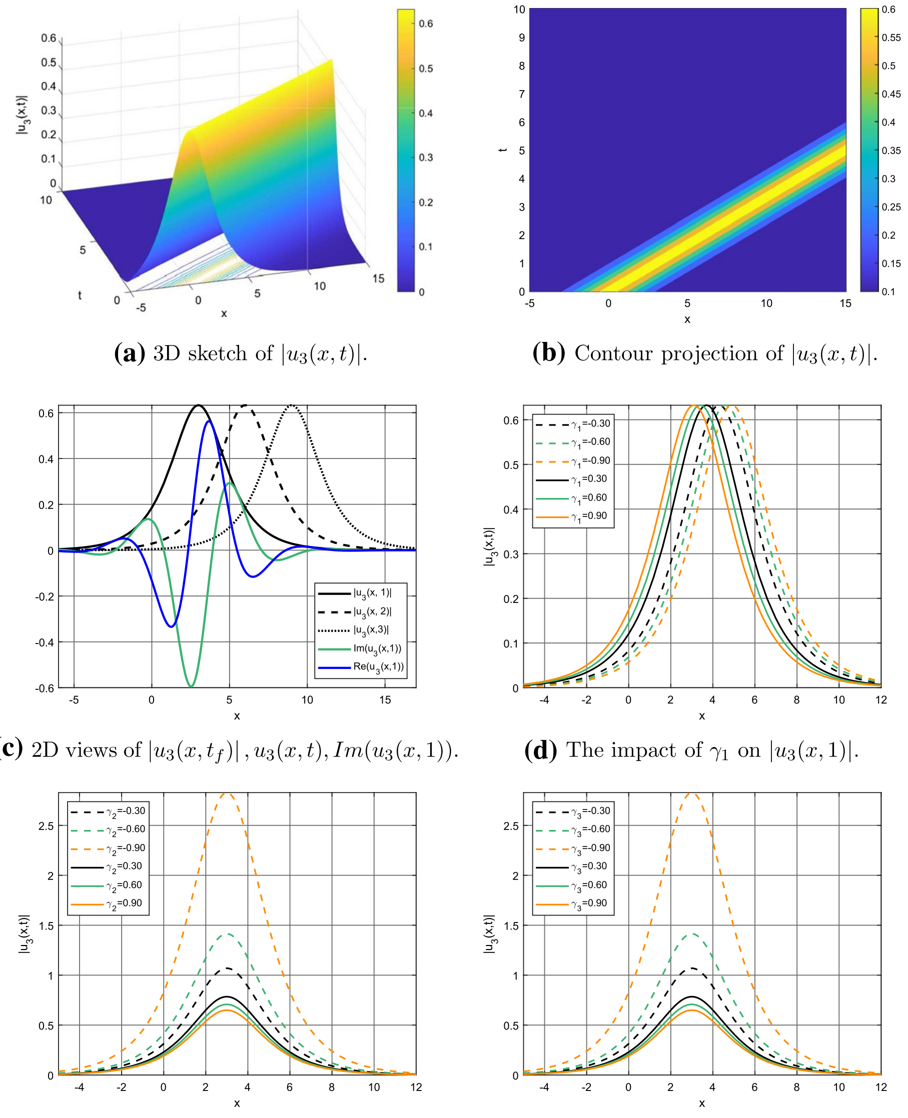

(a) 3D sketch of $|u_3(x,t)|$.

(b) Contour projection of $|u_3(x,t)|$.

(c) 2D views of $|u_3(x,t_f)|, u_3(x,t), Im(u_3(x,1))$.

(d) The impact of γ_1 on $|u_3(x,1)|$.

(e) The impact of γ_2 on $|u_3(x,1)|$.

(f) The impact of γ_3 on $|u_3(x,1)|$.

Fig. 1 Some graphical representations of $u_3(x,t)$ in Eq. (20) by selecting $Cset^1$ in Eq. (17) for the parameters $\gamma = -0.1, \gamma_1 = \gamma_2 = \gamma_3 = \varphi = \eta = 1, \alpha_1 = 2, k = -1$ and the effects of $\gamma_1, \gamma_2, \gamma_3$

solid to dotted lines) represents the bright soliton plot for $|u_3(x,t)|$. From Fig. 1c, it can be seen that the soliton has traveling wave property and moves to the right. Figure 1d is the first graph created to examine the effects of the coefficients $(\gamma_1, \gamma_2, \gamma_3)$ of inter-modal dispersion, the self-steepening and nonlinear dispersion terms on soliton behavior, respectively, which is the main purpose of this study. It is aimed to examine the effect of the γ_1 on the bright soliton presented with Fig. 1a. For this purpose, 0.30, 0.60 and 0.90 values (dotted lines for negative values, solid lines for positive values) are assigned to the coefficients.

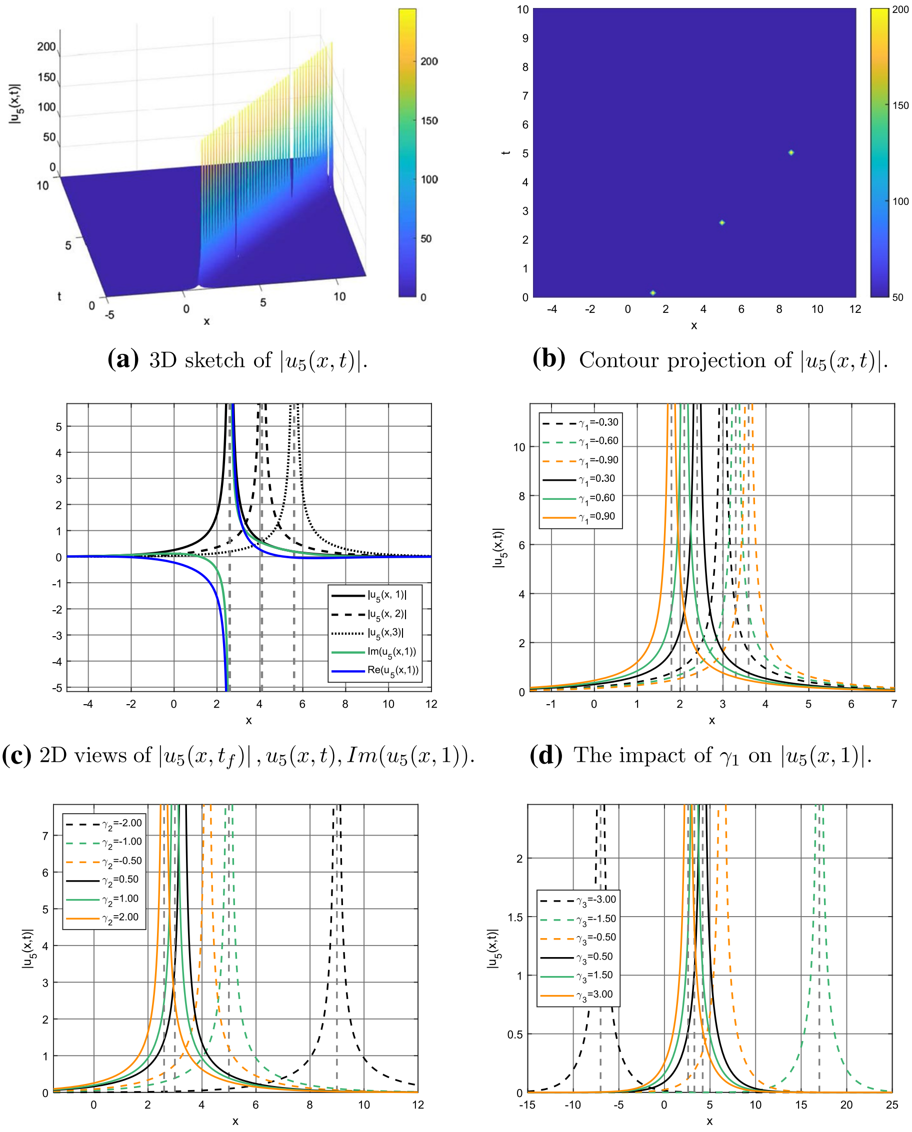

(a) 3D sketch of $|u_5(x,t)|$.

(b) Contour projection of $|u_5(x,t)|$.

(c) 2D views of $|u_5(x,t_f)|, u_5(x,t), Im(u_5(x,1))$.

(d) The impact of γ_1 on $|u_5(x,1)|$.

(e) The impact of γ_2 on $|u_5(x,1)|$.

(f) The impact of γ_3 on $|u_5(x,1)|$.

Fig. 2 Some graphical representations of $u_5(x,t)$ in Eq. (22) by selecting $Cset^2$ in Eq. (17) for the parameters $\gamma=-0.1, \gamma_1=0.1, \gamma_2=2, \gamma_3=3, \alpha_1=2, \eta=1, A_1=1, \varphi=-1$ and the effects of $\gamma_1, \gamma_2, \gamma_3$

From Fig. 1d, it is observed that there is no change in the vertical amplitude of the soliton when the γ_1 is both negative or positive, the soliton maintains its bright soliton character, its skirts remain on the horizontal axis, and the horizontal distance between the soliton's skirts is preserved. When γ_1 is negative and increasing, the soliton changes position to the left depending on the increase in γ_1 (dashed orange to black lines). In case the γ_1 is positive and increasing, the soliton shows a similar position change to the left depending on

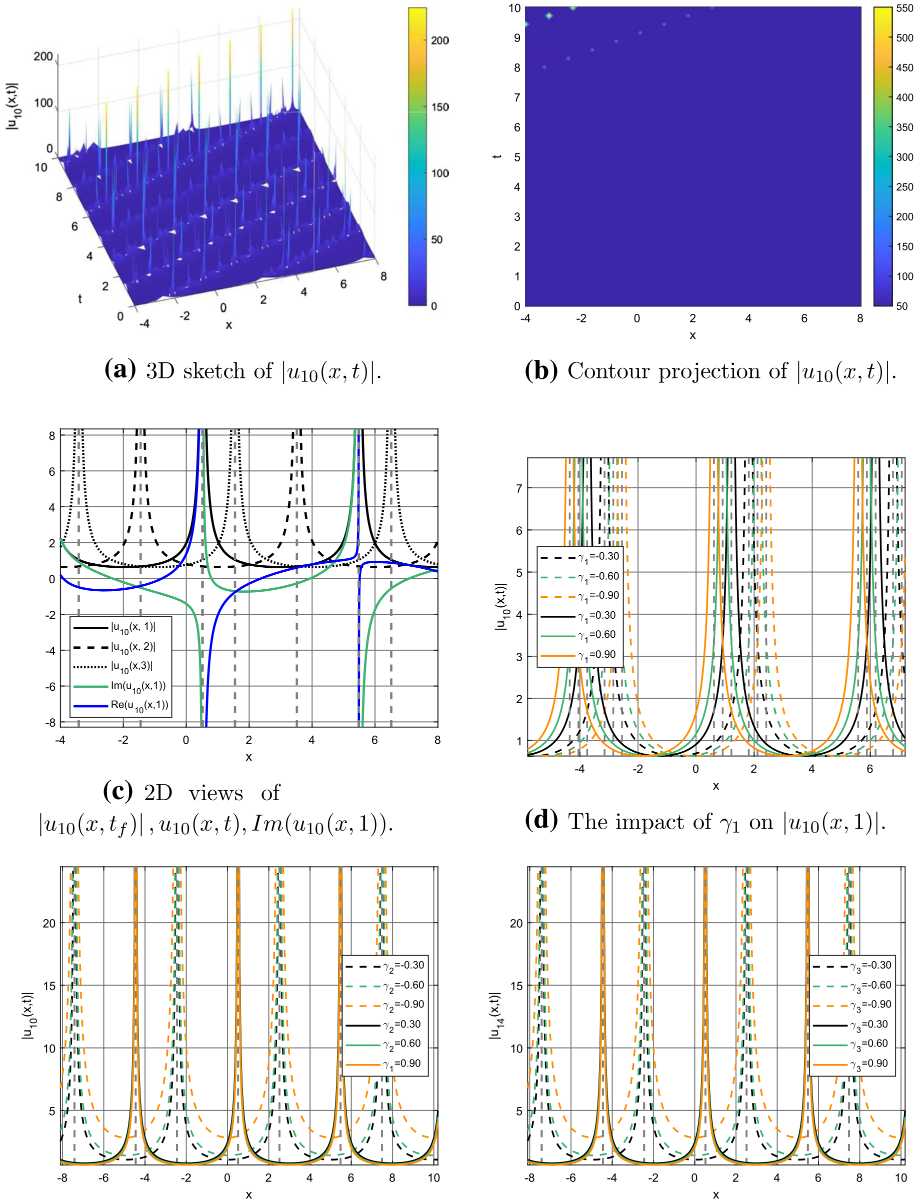

(a) 3D sketch of $|u_{10}(x,t)|$.

(b) Contour projection of $|u_{10}(x,t)|$.

(c) 2D views of $|u_{10}(x,t_f)|, u_{10}(x,t), Im(u_{10}(x,1))$.

(d) The impact of γ_1 on $|u_{10}(x,1)|$.

(e) The impact of γ_2 on $|u_{10}(x,1)|$.

(f) The impact of γ_3 on $|u_{10}(x,1)|$.

Fig. 3 Some graphical representations of $u_{10}(x,t)$ in Eq. (27) by selecting $Cset^1$ in Eq. (17) for the parameters $\gamma = -0.1, \gamma_1 = 0.1, \gamma_2 = 2, \gamma_3 = 3, \alpha_1 = 2, \eta = 1, k = \varphi = -1$ and the effects of $\gamma_1, \gamma_2, \gamma_3$

the increase in γ_1 (solid black to orange lines). Thus, in both cases (γ_1 negative or positive) the coefficient of inter-modal dispersion term has a similar effect on the bright soliton. Figure 1e includes review belongs to γ_2 which is the coefficient of the self-steepening dispersion term. The value for γ_2 is also chosen as 0.30, 0.60 and 0.90 (dotted lines for

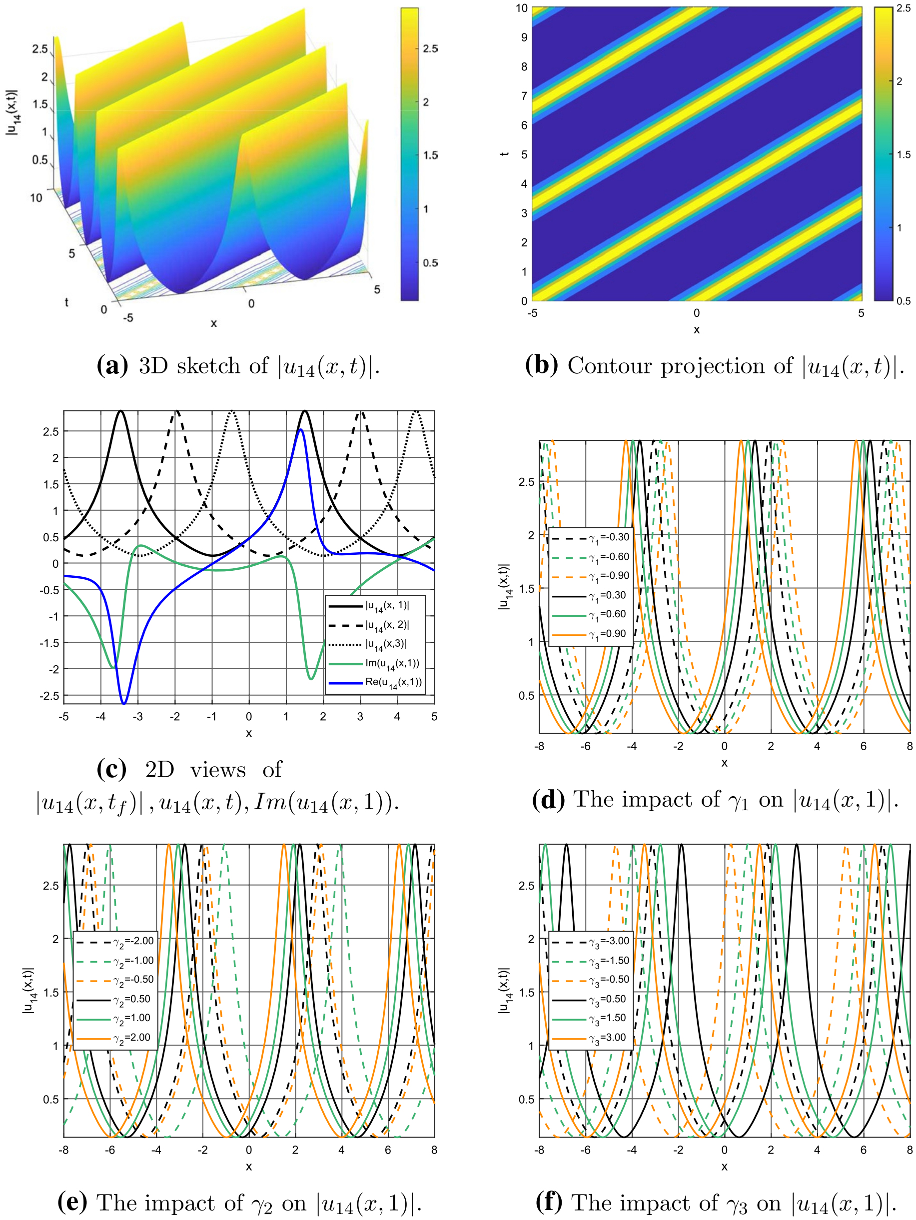

(a) 3D sketch of $|u_{14}(x,t)|$.

(b) Contour projection of $|u_{14}(x,t)|$.

(c) 2D views of $|u_{14}(x,t_f)|, u_{14}(x,t), Im(u_{14}(x,1))$.

(d) The impact of γ_1 on $|u_{14}(x,1)|$.

(e) The impact of γ_2 on $|u_{14}(x,1)|$.

(f) The impact of γ_3 on $|u_{14}(x,1)|$.

Fig. 4 Some graphical representations of $u_{14}(x,t)$ in Eq. (31) by selecting $Cset^3$ in Eq. (17) for the parameters $\gamma = 0.1, \gamma_1 = 1, \gamma_2 = 2, \gamma_3 = 3, \alpha_1 = 2, \eta = 1, k = -1, \varphi = 1$ and the effects of $\gamma_1, \gamma_2, \gamma_3$

negative values, solid lines for positive values). Unlike the previous review, it is seen that the change in the self-steepening dispersion term coefficient has a significant effect on the bright soliton obtained in the Fig. 1a. At first glance, this effect is observed as the change in the vertical amplitude of the soliton. When Fig. 1 is examined in detail, when γ_2 gets negative and increasing values, the soliton maintains its bright soliton character, but there is a change in its vertical amplitude (position of the peak), and this change is observed in the form of a decrease in amplitude (vertical downward displacement of the peak point) depending on its increasing values (dashed orange to black lines). In the case that γ_2 takes positive and increasing values, the soliton maintains its bright soliton character, there is a change in its vertical amplitude (position of the peak), and this change is a decrease in the amplitude (vertical downward displacement of the peak) depending on the increasing values of γ_2 (solid black to orange lines). Therefore, for the self-steepening term coefficient γ_2, if it continues to take increasing values in both cases (negative or positive) for the examined case, the amplitude of the soliton will continue to decrease, in other words, the peak of the soliton will approach the horizontal axis and the soliton will become flattered. We can say that it will evolve into a new appearance, and if the increase in γ_2 continues, the soliton will gradually lose its bright soliton feature. Therefore, in terms of soliton transmission, it has an important effect in terms of preserving the character and amplitude of the soliton signal (soliton pulse) to be transmitted, and it is of great importance to select and control this coefficient depending on the interaction with other nonlinear terms. Figure 1f shows the effect of our analysis for the nonlinear dispersion term coefficient γ_3. If Fig. 1f is examined in detail, we can categorically make similar comments made for γ_2. When γ_3 is both negative and positive, the soliton shows a position change to the left depending on the increasing values of γ_3.

Figure 2 is the graph of the combination of $u_5(x,t)$ in Eq. (22) and $Cset^2$ in Eq. (17) for the parameters $\gamma = -0.1, \gamma_1 = 0.1, \gamma_2 = 2, \gamma_3 = 3, \alpha_1 = 2, \eta = 1, A_1 = 1, \varphi = -1$. Figure 2a–c (black lines) are 3D, contour 2D graphics of $\left|u_5(x,t)\right|$. As in the previous section, $Im(u_5(x,1))$ (blue line), $Re(u_5(x,1))$ (green line) are given by Fig. 2c. All three graphics reflect the singular soliton character. This singularity is up directional ($+\infty$) for both sides of the singular point for $\left|u_5(x,t)\right|$. $Im(u_5(x,1))$ and $Re(u_5(x,1))$ are down directional ($-\infty$) on the left of the singular point, and up directional ($+\infty$) on the right of the singular point. 2d reflects the effect on the singular soliton obtained in Fig. 2a with the inter-modal dispersion term coefficient γ_1. Similarly, the values 0.30, 0.60 and 0.90 are chosen. In both cases of γ_1 (negative or positive), the singular soliton character is preserved and the soliton is shifted to the left depending on the increase. 2e shows the examination of the case where γ_2 is 0.50, 1.00 and 2.00 (dotted lines for negative, solid lines for positive). In case γ_2 is both negative and positive, the soliton shows a position change to the left depending on the increasing values of γ_2. In Fig. 2f, the similar analysis is made for γ_3 for values of 0.50, 1.50 and 3.00. When γ_3 is negative and increasing (dashed lines), the soliton behavior does not show a behavior similar to the previously examined cases. For $\gamma_3 = -3.0$, it is on the far left (dashed black), for $\gamma_3 = -1.5$ it is on the far right (dashed green) and then for $\gamma_3 = -0.5$ it is dashed orange. As it can be seen from the graph, when γ_3 is positive and increasing, it shifts to the left between graphs $\gamma_3 = -3.0$ and $\gamma_3 = -1.5$ with smaller amounts depending on the increasing values of γ_3 (solid black to orange lines). With Fig. 2f, we can attribute this situation, which occurs especially when γ_3 is negative, to the interaction between nonlinear terms in such problems and the difficulty of controlling these terms during this interaction.

Figure 3 is the graph of the combination of $u_{10}(x,t)$ in Eq. (27) and $Cset^1$ in Eq. (17) for the parameters $\gamma = -0.1, \gamma_1 = 0.1, \gamma_2 = 2, \gamma_3 = 3, \alpha_1 = 2, \eta = 1, k = \varphi = -1$ and the effects of $\gamma_1, \gamma_2, \gamma_3$. Figure 3 generally reflects the periodic singular soliton image. The effect of γ_1 is examined in Fig. Fig. 3d, and the soliton shows a position change to the left depending on the increasing values of γ_1, both positive and negative. Figure 3e, f are graphs that reflect the effects of γ_2 and γ_3, respectively. In both graphs, depending on the increasing values (negative or positive) for both γ_2 and γ_3, no horizontal position change is observed for the soliton, but there is a change in its vertical amplitude. It is possible to see this change from the skirt parts of the soliton. When γ_2 and γ_3 are negative and increasing, the amplitude decreases (dashed orange to black lines). And when the parameters are positive, the amplitude decreases. But this effect is observed as a smaller change (solid black to orange lines).

Lastly, Fig. 4 is the graph of the combination of $u_{14}(x,t)$ in Eq. (31) and $Cset^3$ in Eq. (17) for the parameters $\gamma = 0.1, \gamma_1 = 1, \gamma_2 = 2, \gamma_3 = 3, \alpha_1 = 2, \eta = 1, k = -1, \varphi = 1.$ Periodic bright soliton character is generally observed in Fig. 4. Similarly, the graph of Fig. 4d is divided into the effect of γ_1 and when γ_1 is both positive or negative, the position of the solution changes to the left depending on the increasing values of γ_1. Figure 4e shows the effect of γ_2. When γ_2 gets negative and increasing values, there is a change in the horizontal position of the soliton, but this change does not occur regularly (regularly to the left or right) depending on the increasing values of γ_2. Because if the graph of $\gamma_2 = -2.00$ (dashed black line) is on the left, the graph of $\gamma_2 = -1.00$ (dashed green line) is on the right, and the graph of $\gamma_2 = -0.50$ (dashed orange line) is observed between these two graphs. This does not happen when γ_2 takes positive and increasing values (solid black to orange lines). 4f shows the effect of γ_3 and the soliton changes to the left depending on the increasing values of γ_3 when γ_3 is both negative and positive. We would also like to emphasize here that all solution functions obtained between Eqs. (18), (32) satisfy the main equation, Eq. (2), with each solution set given in Eq. (17).

5 Conclusion

The existing studies in the literature focus on obtaining solutions of the perturbed Chen–Lee–Liu equation. In addition to obtaining the soliton solution of the perturbed CLL equation, the main purpose of this work is to investigate the impact of inter-modal, self-steepening, and nonlinear dispersion components on the soliton behavior represented by the considered equation. In this study, we have successfully obtained the bright, singular, periodic singular and periodic bright solitons of the perturbed Chen–Lee–Liu equation by applying the modified extended tanh expansion method. After obtaining the specified soliton types, 2D graphs of soliton behaviors have been drawn by giving different values to the coefficients of these terms in order to examine the effect of each term. It should also be noted that the numerical values given to the coefficients have been assigned to ensure both the limitations of the problem and the method and to preserve the soliton shape obtained within the area of the study. Therefore, making this choice often involves many difficulties and complexities in itself. In this aspect, the investigation of the effect of the inter-modal, self-steepening and nonlinear dispersion terms on soliton behaviors for the perturbed Chen–Lee–Liu equation has not been studied and the results within the scope of this study have not been presented. We believe that the gained results within the scope of the study will be useful for studies on problems modeling many physical phenomena in this area.

Author contributions All parts contained in the research carried out by the authors through hard work and a review of the various references and contributions in the field of mathematics and Applied physics.

Funding No funding for this article.

Availability of data and materials Data sharing is not applicable to this article as no datasets were generated or analyzed during the current study.

Declarations

Competing interests This research received no specific grant from any funding agency in the public, commercial or not-for-profit sectors. The authors did not have any competing interests in this research.

Ethical approval The Corresponding Author, declares that this manuscript is original, has not been published before, and is not currently being considered for publication elsewhere. The Corresponding Author confirms that the manuscript has been read and approved by all the named authors and there are no other persons who satisfied the criteria for authorship but are not listed. I further confirm that the order of authors listed in the manuscript has been approved by all of us. The Corresponding Author is the sole contact for the Editorial process and is responsible for communicating with the other authors about progress, submissions of revisions, and final approval of proofs.

References

AAkbar, M.A., Akinyemi, L., Yao, S.W., Jhangeer, A., Rezazadeh, H., Khater, M.M., Ahmad, H., Inc, M.: Soliton solutions to the Boussinesq equation through sine-Gordon method and Kudryashov method. Res. Phys. **25**, 104228 (2021)

Akinyemi, L., Ullah, N., Akbar, Y., Hashemi, M.S., Akbulut, A., Rezazadeh, H.: Explicit solutions to nonlinear Chen–Lee–Liu equation. Mod. Phys. Lett. B **35**(25), 2150438 (2021)

Ali, K.K., Yokus, A., Seadawy, A.R., Yilmazer, R.: The ion sound and Langmuir waves dynamical system via computational modified generalized exponential rational function. Chaos Solitons Fractals **161**, 112381 (2022)

Alrashed, R., Djob, R.B., Alshaery, A.A., Alkhateeb, S.A., Nuruddeen, R.I.: Collective variables approach to the vector-coupled system of Chen–Lee–Liu equation. Chaos Solitons Fractals **161**, 112315 (2022)

Arnous, A.H., Mirzazadeh, M., Akbulut, A., Akinyemi, L.: Optical solutions and conservation laws of the Chen–Lee–Liu equation with Kudryashov's refractive index via two integrable techniques. In: Waves in Random and Complex Media, pp. 1–17 (2022)

Baskonus, H.M., Osman, M.S., Ramzan, M., Tahir, M., Ashraf, S.: On pulse propagation of soliton wave solutions related to the perturbed Chen–Lee–Liu equation in an optical fiber. Opt. Quantum Electron. **53**(10), 1–17 (2021)

Biswas, A.: Chirp-free bright optical soliton perturbation with Chen–Lee–Liu equation by traveling wave hypothesis and semi-inverse variational principle. Optik **172**, 772–776 (2018)

Biswas, A., Arshed, S.: Optical solitons in presence of higher order dispersions and absence of self-phase modulation. Optik **174**, 452–459 (2018)

Biswas, A., Mirzazadeh, M., Eslami, M., Zhou, Q., Bhrawy, A., Belic, M.: Optical solitons in nano-fibers with spatio-temporal dispersion by trial solution method. Optik **127**(18), 7250–7257 (2016)

Cesar, A., Gomez, S., Roshid, H.O., Inc, M., Akinyemi, L., Rezazadeh, H.: On soliton solutions for perturbed Fokas–Lenells equation. Opt. Quantum Electron. **54**(6), 1–10 (2022)

Chen, H.H., Lee, Y.C., Liu, C.S.: Integrability of nonlinear Hamiltonian systems by inverse scattering method. Phys. Scr. **20**(3–4), 490–492 (1979)

Chen, H.H., Lee, Y.C., Lin, J.E.: On the direct construction of the inverse scattering operators of integrable nonlinear Hamiltonian systems. Physica D **26**(1), 165–170 (1987)

Chen, J.S., Hu, W., Puso, M.: Orbital HP-Clouds for solving Schrödinger equation in quantum mechanics. Comput. Methods Appl. Mech. Eng. **196**(37–40 SPEC. ISS.), 3693–3705 (2007)

Cinar, M., Onder, I., Secer, A., Bayram, M., Abdulkadir Sulaiman, T., Yusuf, A.: Solving the fractional Jaulent–Miodek system via a modified Laplace decomposition method. In: Waves in Random and Complex Media, pp. 1–14 (2022a)

Cinar, M., Onder, I., Secer, A., Yusuf, A., Sulaiman, T.A., Bayram, M., Aydin, H.: Soliton Solutions of (2 + 1) dimensional Heisenberg ferromagnetic spin equation by the extended rational sine–cosine and sinh–cosh method. Int. J. Appl. Comput. Math. **7**(4), 135 (2021)

Cinar, M., Onder, I., Secer, A., Bayram, M., Yusuf, A., Sulaiman, T.A.: A comparison of analytical solutions of nonlinear complex generalized Zakharov dynamical system for various definitions of the differential operator. Electron. Res. Arch. **30**(1), 335–361 (2022b)

Do Ó, J.M., Moameni, A., Severo, U.: Semi-classical states for quasilinear Schrödinger equations arising in plasma physics. Commun. Contemp. Math. **11**(4), 547–583 (2009)

Dörfler, W., Lechleiter, A., Plum, M., Schneider, G., Wieners, C.: The role of the nonlinear Schrödinger equation in nonlinear optics. In: Photonic Crystals: Mathematical Analysis and Numerical Approximation, pp. 127–162. Springer, Basel (2011)

Esen, H., Ozdemir, N., Secer, A., Bayram, M.: On solitary wave solutions for the perturbed Chen–Lee–Liu equation via an analytical approach. Optik **245**, 167641 (2021)

Feng, B.-F.: An integrable coupled short pulse equation. J. Phys. A Math. Theor. **45**(8), 085202 (2012)

Gadzhiev, I.T., Gerdzhikov, V.S., Ivanov, M.I.: Hamiltonian structures of nonlinear evolution equations connected with a polynomial pencil. J. Sov. Math. **34**(5), 1923–1932 (1986)

Guo, L., Zhang, Y., Shuwei, X., Zhiwei, W., He, J.: The higher order rogue wave solutions of the Gerdjikov–Ivanov equation. Phys. Scr. **89**(3), 035501 (2014)

Hussain, A., Jhangeer, A., Tahir, S., Chu, Y.-M., Khan, I., Sooppy Nisar, K.: Dynamical behavior of fractional Chen–Lee–Liu equation in optical fibers with beta derivatives. Res. Phys. **18**, 103208 (2020)

Ismael, H.F., Seadawy, A., Bulut, H: Construction of breather solutions and N-soliton for the higher order dimensional Caudrey–Dodd–Gibbon–Sawada–Kotera equation arising from wave patterns. Int. J. Nonlinear Sci. Numer. Simul. (2021)

Ismael, H.F., Bulut, H., Osman, M.S.: The N-soliton, fusion, rational and breather solutions of two extensions of the (2+1)-dimensional Bogoyavlenskii–Schieff equation. Nonlinear Dyn. **107**(4), 3791–3803 (2022)

Korkmaz, A., Hepson, O.E., Hosseini, K., Rezazadeh, H., Eslami, M.: Sine-Gordon expansion method for exact solutions to conformable time fractional equations in RLW-class. J. King Saud Univ. Sci. **32**(1), 567–574 (2020)

Kudryashov, N.A.: General solution of the traveling wave reduction for the perturbed Chen–Lee–Liu equation. Optik **186**, 339–349 (2019)

Kudryashov, N.A.: Optical solitons of the Chen–Lee–Liu equation with arbitrary refractive index. Optik **247**, 167935 (2021)

Leble, S., Reichel, B.: Coupled nonlinear Schrödinger equations in optic fibers theory. Eur. Phys. J. Spec. Top. **173**(1), 5–55 (2009)

Lee, J.H., Pashaev, O.K., Rogers, C., Schief, W.K.: The resonant nonlinear Schrödinger equation in cold plasma physics. Application of Bäcklund–Darboux transformations and superposition principles. J. Plasma Phys. **73**(2), 257–272 (2007)

Liu, X., Triki, H., Zhou, Q., Liu, W., Biswas, A.: Analytic study on interactions between periodic solitons with controllable parameters. Nonlinear Dyn. **94**(1), 703–709 (2018)

Liu, S.-Z., Zhang, Y.-S., He, J.-S.: Smooth positons of the second-type derivative nonlinear Schrödinger equation. Commun. Theor. Phys. **71**(4), 357 (2019)

Mahak, N., Akram, G.: Extension of rational sine-cosine and rational sinh–cosh techniques to extract solutions for the perturbed NLSE with Kerr law nonlinearity. Eur. Phys. J. Plus **134**(4), 1–10 (2019)

Mohamed, M.S., Akinyemi, L., Najati, S.A., Elagan, S.K.: Abundant solitary wave solutions of the Chen–Lee–Liu equation via a novel analytical technique. Opt. Quantum Electron. **54**(3), 1–14 (2022)

Ohsumi, A.: An interpretation of the Schrödinger equation in quantum mechanics from the control-theoretic point of view. Automatica **99**, 181–187 (2019)

Ozdemir, N., Esen, H., Secer, A., Bayram, M., Yusuf, A., Sulaiman, T.A.: Optical soliton solutions to Chen Lee Liu model by the modified extended tanh expansion scheme. Optik **245**, 167643 (2021)

Ozisik, M., Bayram, M., Secer, A., Cinar, M., Yusuf, A., Sulaiman, T.A.: Optical solitons to the (1+2)-dimensional Chiral non-linear Schrödinger equation. Opt. Quantum Electron. **54**(9), 1–13 (2022a)

Ozisik, M., Cinar, M., Secer, A., Bayram, M.: Optical solitons with Kudryashov's sextic power-law nonlinearity. Optik **261**, 169202 (2022b)

Raslan, K.R., Ali, K.K., Shallal, M.A.: The modified extended tanh method with the Riccati equation for solving the space–time fractional EW and MEW equations. Chaos Solitons Fractals **103**, 404–409 (2017)

Sakovich, A., Sakovich, S.: The short pulse equation is integrable. J. Phys. Soc. Jpn. **74**(1), 239–241 (2005)

Shuwei, X., He, J., Wang, L.: The Darboux transformation of the derivative nonlinear Schrödinger equation. J. Phys. A Math. Theor. **44**(30), 305203 (2011)

Tala-Tebue, E., Djoufack, Z.I., Kamdoum-Tamo, P.H., Kenfack-Jiotsa, A.: Cnoidal and solitary waves of a nonlinear Schrödinger equation in an optical fiber. Optik **174**, 508–512 (2018)

Tariq, K.U., Seadawy, A.R., Younis, M.: Explicit, periodic and dispersive optical soliton solutions to the generalized nonlinear Schrödinger dynamical equation with higher order dispersion and cubic-quintic nonlinear terms. Opt. Quant. Electron. **50**(3), 1–19 (2018)

Tariq, K.U., Zainab, H., Seadawy, A.R., Younis, M., Rizvi, S.T.R., Mousa, A.A.A.: On some novel optical wave solutions to the paraxial M-fractional nonlinear Schrödinger dynamical equation. Opt. Quantum Electron. **53**(5), 1–14 (2021)
Tariq, K.U., Seadawy, A.R., Zainab, H., Ashraf, M.A., Rizvi, S.T.R.: Some new optical dromions to (2+1)-dimensional nonlinear Schrödinger equation with Kerr law of nonlinearity. Opt. Quantum Electron. **54**(6), 1–16 (2022)
Tariq, K.U., Wazwaz, A.-M., Ahmed, A.: On some optical soliton structures to the Lakshmanan–Porsezian–Daniel model with a set of nonlinearities. Opt. Quant. Electron. **54**(7), 1–34 (2022)
Tarla, S., Ali, K.K., Yilmazer, R., Osman, M.S.: On dynamical behavior for optical solitons sustained by the perturbed Chen–Lee–Liu model. Commun. Theor. Phys. **74**(7), 075005 (2022)
Tarla, S., Ali, K.K., Yilmazer, R., Osman, M.S.: The dynamic behaviors of the Radhakrishnan–Kundu–Lakshmanan equation by Jacobi elliptic function expansion technique. Opt. Quantum Electron. **54**(5), 1–12 (2022)
Tarla, S., Ali, K.K., Yilmazer, R., Osman, M.S.: New optical solitons based on the perturbed Chen–Lee–Liu model through Jacobi elliptic function method. Opt. Quantum Electron. **54**(2), 1–12 (2022)
Trulsen, K., Kliakhandler, I., Dysthe, K.B., Velarde, M.G.: On weakly nonlinear modulation of waves on deep water. Phys. Fluids **12**(10), 2432–2437 (2000)
Tsuchida, T., Wadati, M.: New integrable systems of derivative nonlinear Schrödinger equations with multiple components. Phys. Lett. A **257**(1), 53–64 (1999)
Xia, W., Ma, Y., Dong, G., Zhang, J., Ma, X.: Emergence of solitons from irregular waves in deep water. J. Mar. Sci. Eng. **9**(12), 1369 (2021)
Yépez-Martínez, H., Rezazadeh, H., Inc, M., Ali Akinlar, M. New solutions to the fractional perturbed Chen–Lee–Liu equation with a new local fractional derivative. In: Waves in Random and Complex Media, pp. 1–36 (2021)
Yildirim, Y.: Optical solitons to Chen–Lee–Liu model in birefringent fibers with trial equation approach. Optik **183**, 881–886 (2019)
Yildirim, Y., Biswas, A., Asma, M., Ekici, M., Ntsime, B.P., Zayed, E.M., Moshokoa, S.P., Alzahrani, A.K., Belic, M.R.: Optical soliton perturbation with Chen–Lee–Liu equation. Optik **220**, 165177 (2020)
Yin, J., Duan, X., Tian, L.: Optical secure communication modeled by the perturbed nonlinear Schrödinger equation. Opt. Quant. Electron. **49**(10), 1–11 (2017)
Yokus, A., Durur, H., Duran, S.: Simulation and refraction event of complex hyperbolic type solitary wave in plasma and optical fiber for the perturbed Chen–Lee–Liu equation. Opt. Quant. Electron. **53**(7), 1–17 (2021)
Yusuf, A., Inc, M., Aliyu, A.I., Baleanu, D.: Optical solitons possessing beta derivative of the Chen–Lee–Liu equation in optical fibers. Front. Phys. **7** (2019)
Zhang, Y., Guo, L., He, J., Zhou, Z.: Darboux transformation of the second-type derivative nonlinear Schrödinger equation. Lett. Math. Phys. **105**(6), 853–891 (2015)
Zhang, Y., Dong, H., Fang, Y.: The multicomponent higher-order Chen–Lee–Liu system: the Riemann–Hilbert Problem and its N-soliton solution. Fractal Fract. **6**(6), 327 (2022)
Zhou, S., Liu, J., Chen, S., Yao, Y.: The nth-Darboux transformation and explicit solutions of the PT-symmetry second-type derivative nonlinear Schrödinger equation. J. Nonlinear Math. Phys. **29**, 573–587 (2022)
Zhou, Q.: Analytical solutions and modulation instability analysis to the perturbed nonlinear Schrödinger equation. J. Mod. Opt. **61**(6), 500–503 (2014)

Publisher's Note Springer Nature remains neutral with regard to jurisdictional claims in published maps and institutional affiliations.